

# Blunted arterial baroreflex causes “pathological” heart rate turbulence

RALF MROWKA,<sup>1</sup> PONTUS B. PERSSON,<sup>1</sup> HEINZ THERES,<sup>2</sup> AND ANDREAS PATZAK<sup>1</sup>

<sup>1</sup>Johannes-Müller-Institut für Physiologie, Charité, Humboldt-Universität zu Berlin and <sup>2</sup>Klinik für Innere Medizin I, Charité, Kardiologie, D-10117 Berlin, Germany

Received 27 January 2000; accepted in final form 20 April 2000

**Mrowka, Ralf, P. B. Persson, H. Theres, and A. Patzak.** Blunted arterial baroreflex causes “pathological” heart rate turbulence. *Am J Physiol Regulatory Integrative Comp Physiol* 279: R1171–R1175, 2000.—Sudden cardiac death is the leading cause of cardiovascular mortality in developed countries. Recently, two post-myocardial-infarction risk predictors were introduced that are superior to all other presently available indicators: turbulence onset (TO) and turbulence slope (TS). These parameters characterize the behavior of instantaneous heart rate after a ventricular premature beat, i.e., they describe the reestablishing of heart rate control after an acute perturbation. We propose that the dysfunction of an important cardiovascular control mechanism, the arterial baroreflex, is the mechanism behind these new potent markers. The hypothesis is tested by means of a physiological model involving the excitation generation in the heart, the hemodynamic situation in the aorta, and baroreceptor feedback mechanisms. The data show that a blunted baroreceptor response of the heart resembles patterns of heart rate turbulence that correspond to pathological values of TO and TS. The results of the model suggest that the recently established risk parameters TO and TS characterize baroreflex function, a known risk stratifier in patients.

sudden cardiac death; risk factors; baroreceptors; model

SUDDEN CARDIAC DEATH (SCD) is the leading cause of cardiovascular mortality in developed countries (9). There are a number of diagnostic parameters such as low left ventricular (VE) ejection fraction (8), low heart rate variability (3), abnormal signal-averaged electrocardiograms (14) and t wave alternans (12), which, if present, indicate an increased risk for SCD.

Decreased baroreflex function has been observed in patients at risk for SCD in a number of studies (1, 4). Reasons for this regulatory malfunction may be found in an altered baroreceptor sensitivity, modified central processing, or a decreased response of the heart. The latter is consistent with the finding that decreased heart rate variability (HRV) is correlated with higher mortality (16). Recently, two post-myocardial-infarction risk predictors were introduced that are stronger than all other presently available indicators: turbulence onset (TO) and tur-

bulence slope (TS) (15). These parameters characterize the behavior of instantaneous heart rate after a VE premature beat (VPB).

A VPB with a compensatory pause leads to a drop in arterial blood pressure. Therefore, baroreflex action is essential in the compensation of blood pressure. It has been claimed (15), however, that the absence of heart rate turbulence after VPB is independent of other known risk factors. The question arises as to whether this is true, i.e., if there may be a link between the new stratifiers TS and TO and the baroreflex function.

A standard therapy scheme after myocardial infarction (13) includes  $\beta_1$ -adrenoceptor blockade. The effect of this medication on the new parameters is not known.

## METHODS

*Modeling the physiological situation.* Heart rate rhythmicity is maintained by excitatory signals within the heart. The heartbeat is initiated in the sinoatrial (SA) node. The excitation propagates through the conducting system across the atrioventricular (AV) node, reaching finally the Purkinje fibers in the two ventricles. If, for any reason (e.g., sick sinus syndrome or SA block), the SA node fails to generate the primary excitation, the AV node substitutes the excitation as a secondary pacemaker. Moreover, there is an additional “life saver.” If there is a complete AV block or if the AV node fails to generate the secondary rhythm, a tertiary center in the VE conducting tissue takes over pacing. This physiological situation was implemented in a model using three oscillators, each having its own natural frequency corresponding to the physiological correlate.

Each oscillator transits through three states, slow depolarization up to a threshold, fast depolarization, and repolarization. The three oscillators are coupled with a time delay for conductance. Thus, when one oscillator reaches fast depolarization, it pulls the neighboring oscillator to fast depolarization, provided this nearby oscillator is in the state of slow depolarization. The SA node is the primary pacemaker because it has the highest pacemaker frequency.

The second part of the model simulates the pressure in the aorta by means of a windkessel (7, 11, 17). This hemodynamic component reflects cardiac output volume being pumped into a compliant system, the aorta. The pressure within this vessel is proportional to its volume. Furthermore, aortic outflow is proportional to the pressure and is controlled by peripheral resistance.

The third modeling element describes arterial baroreflex function (2, 10). The baroreceptors are located in large-

R. Mrowka, Johannes-Müller-Institut für Physiologie, Charité, Humboldt-Universität zu Berlin, Tucholskystr. 2, D-10117 Berlin, Germany (E-mail: ralf.mrowka@charite.de)

conduit arteries. When the wall of these vessels is distended, baroreceptor discharge increases. Cardioinhibitory centers in the central nervous system sense baroreceptor output, thus enhancing parasympathetic tone and inhibiting sympathetic output to the heart. As a result, heart rate and blood pressure decrease. This reflex-loop is sluggish, hence, time delays were added for the parasympathetic and the sympathetic responses (6). In the model, autonomic activation tapers off according to a first-order kinetic process, with a shorter half time for the parasympathetic effects compared with the half time of the sympathetic decay. Modulation of heart rate by the autonomic system in this model occurs by influencing the transition time for depolarization of the sinus node.

**Experiments.** Two experiments were performed. First, baroreceptor sensitivity (BRS) was attenuated in steps. The risk parameters TO and TS were calculated for each step by inducing a spontaneous VE beat in the model. The second experiment takes into account the attenuation of nerve traffic to the heart, as achieved by  $\beta_1$ -adrenoceptor blockade, one of the standard therapy schemes (13) after myocardial infarction.

TO and TS are the two stratifiers described in the recent work of Schmidt and colleagues (15). They defined turbulence onset as the difference between the mean of the first two sinus R-R intervals after a VPB and the mean of the last two sinus R-R intervals before the VPB divided by the mean of the latter. Turbulence slope was determined within the first 20 sinus-rhythm intervals after a VPB. To this end, the maximum positive slope of a linear regression line was assessed over any sequence of five subsequent sinus rhythm R-R intervals.

## RESULTS

In the model, reduction of the BRS induced patterns of R-R intervals after VPB with a striking similarity to patterns found in patients at high risk for sudden cardiac death (Fig. 1, C and E). Conversely, intact BRS yielded patterns corresponding to low-risk patients (Fig. 1, D and F).

The relationship of the turbulence parameters vs. BRS is shown in Fig. 2. Reduced BRS, as often found in high-risk patients after myocardial infarction, markedly affected TS and TO. These results are consistent with the finding that an attenuated baroreceptor sensitivity increases the risk for SCD (4).

In the second experiment, a reduced cardiac sympathetic response (e.g., as under treatment with  $\beta_1$ -adrenoceptor antagonists) dramatically changed the dependency of the risk marker TS on BRS. This finding may explain why the combination of TS and TO improve the estimation of the relative risk in the study conducted by Schmidt et al. (15). Variables and constants may be found in Table 1.

## DISCUSSION

The mathematical model presented in this study describes the evolution of heart rate after a VPB. For the excitation process, the hemodynamic components, as well as for the feedback part, simple assumptions were made. The model is capable of producing normal and pathological patterns after VPB as typically seen in patients (Fig. 1) (15). The model predicts that the

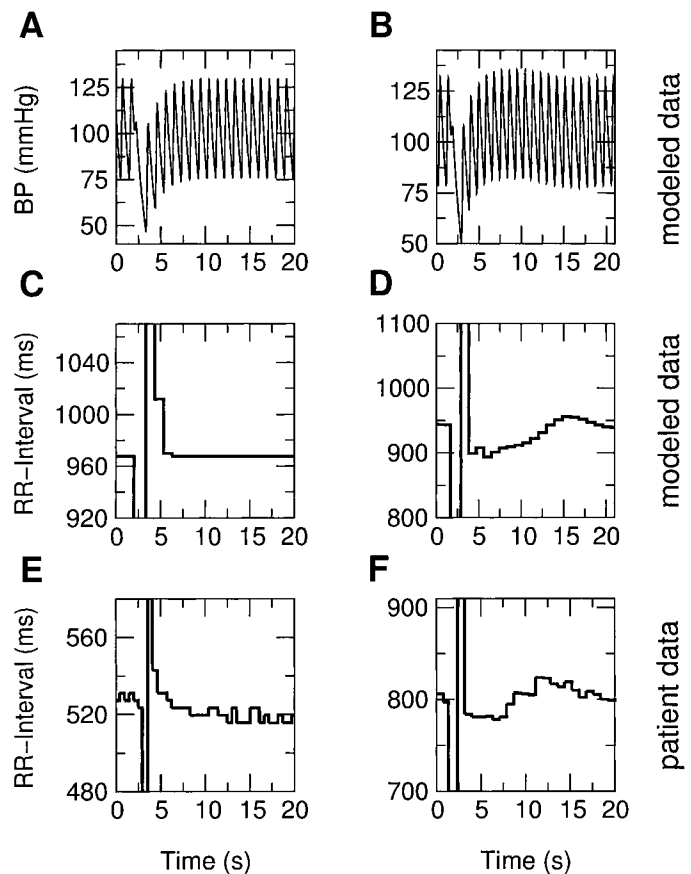


Fig. 1. Effect of ventricular premature beats on modeled blood pressure (BP; A, B), on modeled heart rate (C, D), and on heart rate in patients (E, F). A blunted baroreceptor response is simulated in A and C, whereas B and D refer to data modeled for a normal baroreceptor response. The pattern in C corresponds to those observed in patients at high risk for sudden cardiac death (E). The trace in E was recorded 5 min before a life-threatening ventricular arrhythmia in a 59-yr-old female patient (dilatative cardiomyopathy, data derived from an implantable cardiac defibrillator). The response characteristics of the simulation in D resemble those of low-risk patients, as shown as an individual example in F (55-yr-old male subject, no history of cardiac pathology).

parameter TO, which refers to the early acceleration of heart rate, is not affected as much by  $\beta_1$ -adrenoceptor antagonists as the parameter TS. This is mainly due to the fact that the nonaffected parasympathetic modulation of heart rate is rapid compared with the "sluggish" sympathetic effect.

Of course, models in general may only partially describe all components involved. For instance, the neural control of the heart is extremely complex, and the contribution of the sympathetic and parasympathetic nervous system is not a simple algebraic sum (5). Our model recognizes this fact, i.e., that each contribution of neural activity may not be infinitely large. This is due to the use of a tanh transfer function, introducing a nonlinear component at this stage.

The simulation results suggest a strong link between the new stratifiers TS and TO and the arterial baroreflex (Fig. 2). Therefore, the recently established risk stratifiers TO and TS are not independent of the al-

ready known risk factor “lowered baroreceptor sensitivity” (4).

One common approach to study a system is to perturb it by an impulse and then to analyze the impulse response. A VPB is a naturally occurring experiment of this kind. Provided the system is healthy, it shows a normal characteristic pattern of heart rate turbulence.

### Perspectives

New strategies for estimating cardiovascular risk are of mutual importance. Here, we have presented a mathematical model that may be used to gain further insight into the importance of TS and TO. The complex dynamical properties of blood pressure and heart rate are not reliably anticipated visually, i.e., without nu-

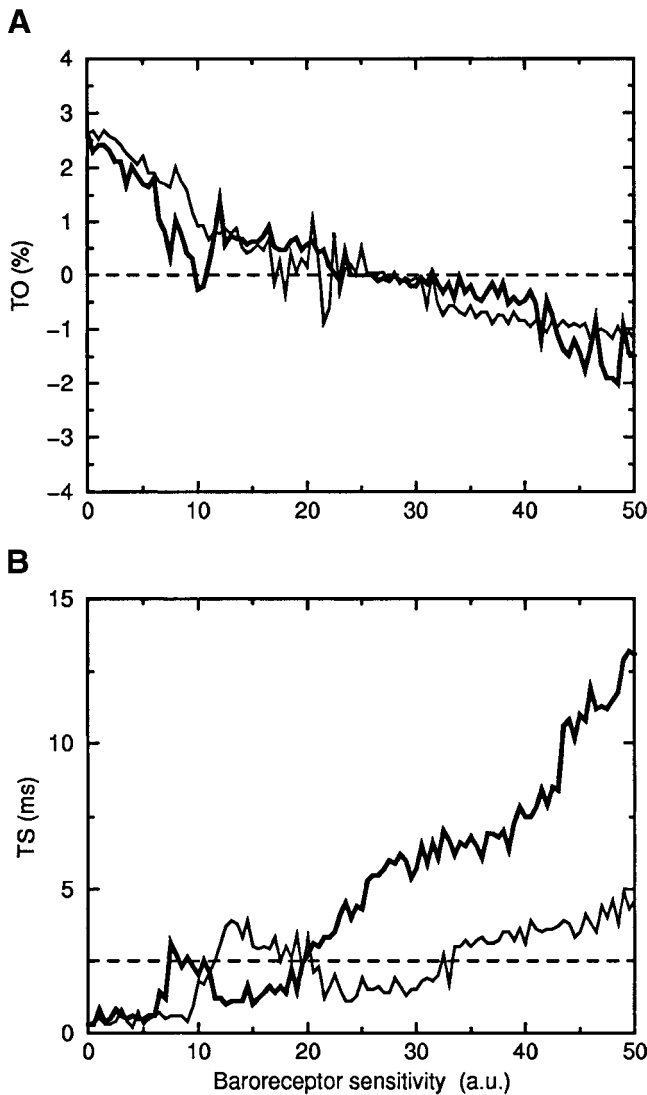


Fig. 2. Results for the risk parameters. Turbulence onset (A) and turbulence slope (B), as a function of the baroreceptor sensitivity of the heart (bold lines). The thin lines correspond to  $\beta_1$ -adrenoceptor blockade. The horizontal lines (dashed) indicate the cut-off values below which (A) and above which (B) “normal” values are expected. a.u., arbitrary units; TO, turbulence onset; TS, turbulence slope.

Table 1. *Variables and constants*

Name	Description	Value (unit; adopted from)
$U_X$	potential in structure $X$	variable (mV)
$c_{SA}^i$	de- and repolarization constant	180, 1,200, -128 (mV/s)
$c_{AV}^i$	"	110, 1,200, -128 (mV/s)
$c_{VE}^i$	"	65, 1,200, -128 (mV/s)
$T_n$	thresholds for state transitions	-30, 20, -70 (mV)
$dIn/dt$	influx in aorta from ventricle	variable (l/s)
$dOut/dt$	outflux from aorta	variable (l/s)
$P_{Aorta}$	blood pressure in aorta	variable (mmHg)
$V_{Aorta}$	blood volume in aorta	variable (l)
$compl_{Aorta}$	compliance of aorta	0.00125 (l/mmHg; Ref. 11)
$EjVolume$	ejection volume	0.08 (l)
$t_{EjStart}$	time of ejection start	variable (s)
$t_{EjTime}$	time for ejection	0.27 (s; Ref. 11)
$res_{peri}$	peripheral resistance	1068 (mmHg $\times$ s/l; Ref. 11)
Sym	sympathetic tone	variable
Ach	parasympathetic tone	variable
$K_{sym}, K_{Ach}$	sensing scaling factor	0.3, 0.3
$P_{const}$	sensing level	120 (mmHg)
$deg_{sym}, deg_{Ach}$	degrading constants	0.239, 2.0
$\tau_{Sym}, \tau_{Ach}$	time delay	2.5, 0.5 (s; Ref. 6)
$o_{Sym}, o_{Ach}$	transfer offset	20, 15
$f_{Sym}, f_{Ach}$	transfer factor	0.25
Block	adrenoceptor blockade factor	$\begin{cases} 1 & \text{for normal} \\ 0.5 & \text{for blockade} \end{cases}$
BRS	baroreceptor sensitivity	0-50
$t$	time	variable (s)

Variables and constants for equations of the model described in APPENDIX.

merical simulation. Our model suggests that TS and TO may not be novel independent risk stratifiers. They rather seem to reflect baroreceptor sensitivity. It would be appropriate to validate the model prediction with the data of the autonomic tone and reflexes after myocardial infarction trial (4), in which the turbulence parameters TO and TS can readily be calculated from the holter tapes that were recorded during the study.

### APPENDIX

#### Description of the Model Properties

*Generation of rhythms.* The rhythmicity-generating component of the model consists of three oscillators analogous to the SA node, the AV node, and (VE) tissue. Each oscillator repeatedly passes through three states (0, 1, 2), corresponding to slow depolarization, depolarization, and repolarization. The  $c_X$  determines the natural frequency of the oscillator  $X$ . The SA node is modulated by autonomic tone, which resulting component is  $cmod$ . A state transition for state  $X = n$  to the following state occurs if potential ( $U$ ) has reached a threshold ( $T_n$ ).

Oscillator in SA node

$$\frac{dU_{SA}}{dt} = \begin{cases} c_{SA}^0 + cmod & \text{if } state_{SA} = 0 \\ c_{SA}^1 + cmod & \text{if } state_{SA} = 1 \\ c_{SA}^2 & \text{if } state_{SA} = 2 \end{cases}$$

Oscillator AV node

$$\frac{dU_{AV}}{dt} = c_{AV}^i \quad \text{for } state_{AV} = i \quad i \in \{0, 1, 2\}$$

Oscillator in the ventricle

$$\frac{dU_{VE}}{dt} = c_{VE}^i \quad \text{for } state_{VE} = i \quad i \in \{0, 1, 2\}$$

Excitation in oscillator  $X$ , defined as  $state_X = 1$ , can reach to neighboring oscillators  $SA \rightleftharpoons AV$  and  $AV \rightleftharpoons VE$  in either direction with a delay of  $\tau$ . This coupling was achieved by setting the state of oscillators  $X$ ,  $state_X$ , to the value of 1 if this oscillator is in  $state_X = 0$  (slow depolarization) and there was a transition from 0 to 1 at time  $t - \tau$  in the neighboring oscillator [de- and repolarization constants ( $c^i$ )].

*Hemodynamic part.* The implementation of the hemodynamic component included a windkessel (11). When the ventricular oscillator VE reaches the depolarization state, the volume is pumped into the aorta. This is accomplished in the model by setting  $t_{EjStart} = 0$ . This incorporates the feed-forward from heart rate to blood pressure. The outflux is proportional to aortic pressure and is controlled by peripheral resistance. The compliance of the aorta determines the relationship between pressure and volume.

Influx

$$\frac{dIn}{dt} = \frac{EjVolume \times \pi}{2 \times t_{EjTime}} \sin [\pi(t - t_{EjStart})/t_{EjTime}]$$

$$\text{for } (t - t_{EjStart}) < t_{EjTime}$$

Outflux

$$\frac{dOut}{dt} = P_{Aorta}/res_{peri}$$

Pressure

$$P_{Aorta} = V_{Aorta}/compl_{Aorta}$$

Volume

$$\frac{dVolume_{Aorta}}{dt} = \frac{dIn}{dt} - \frac{dOut}{dt}$$

(For variables and constants, see Table 1.)

*Baroreceptor feedback.* Baroreceptors located in the conduit arteries “measure” the pressure; their discharge is pressure dependent. When pressure increases, parasympathetic tone (Ach) is enhanced and sympathetic tone (Sym) is diminished. There is a time delay for this feedback,  $\tau_{Ach}$  and  $\tau_{Sym}$ , for the parasympathetic and sympathetic response, respectively (6). Parasympathetic tone decelerates, and sympathetic activity accelerates the frequency of the SA node. Autonomic activity tapers off according to a first-order process determined by  $deg_x$ . The sensitivity of the heart to this baroreceptor feedback loop is characterized by BRS. The net effect of the autonomic tone on the SA node is  $cmod$ . Adrenoceptor blockade was simulated by decreasing the sympathetic influence. This was achieved reducing block from 1 to 0.5.

Sympathetic tone

$$\frac{dSym}{dt} = K_{sym}[P_{Const} - P_{Aorta}(t - \tau_{sym})] - Sym \times deg_{sym}$$

Parasympathetic tone

$$\frac{dAch}{dt} = K_{Ach}[P_{Aorta}(t - \tau_{Ach})] - Ach \times deg_{Ach}$$

Net effect

$$cmod = BRS[f_{Ach} \tanh(o_{Ach} - Ach) + block \times f_{Sym} \tanh(Sym - o_{sym})]$$

(For variables and constants, see Table 1.)

*Induction of VPB.* After an equilibrium phase of 33 normal beats, VPB were induced in the ventricle by setting  $state_{VE}$  to 1 at 0.5 s after the last start of excitation in the ventricle. The ejection volume resulting from VPB was assumed to be  $\frac{1}{4}$  of normal.

This work was supported by “Deutsche Forschungsgemeinschaft.”

## REFERENCES

1. **Billman GE, Schwartz PJ, and Stone HL.** Baroreceptor reflex control of heart rate: a predictor of sudden cardiac death. *Circulation* 66: 874–880, 1982.
2. **Hering HE.** *Die Karotissinusreflexe auf Herz und GefäÙe.* Dresden-Leipzig, Germany: Steinkopff Verlag, 1927.
3. **Hohnloser SH, Klingenhoben T, Zabel M, and Li YG.** Heart rate variability used as an arrhythmia risk stratifier after myocardial infarction. *Pacing Clin Electrophysiol* 20: 2594–2601, 1997.
4. **La Rovere MT, Bigger JT Jr, Marcus FI, Mortara A, and Schwartz PJ.** Baroreflex sensitivity and heart-rate variability in prediction of total cardiac mortality after myocardial infarction. ATRAMI (Autonomic Tone and Reflexes After Myocardial Infarction) investigators. *Lancet* 351: 478–484, 1998.
5. **Levy MN.** Sympathetic-parasympathetic interactions in the heart. *Circ Res* 29: 437–445, 1971.
6. **Madwed JB, Albrecht P, Mark RG, and Cohen RJ.** Low-frequency oscillations in arterial pressure and heart rate: a simple computer model. *Am J Physiol Heart Circ Physiol* 256: H1573–H1579, 1989.
7. **Marey EJ.** *La Circulation Du Sang. A L'état Physiologique et Dans Les maladies.* Paris: Masson, 1881.
8. **Multicenter Postinfarction Research Group.** Risk stratification and survival after myocardial infarction. *N Engl J Med* 309: 331–336, 1983.
9. **Myerburg RJ, Interian A Jr, Mitrani RM, Kessler KM, and Castellanos A.** Frequency of sudden cardiac death and profiles of risk. *Am J Cardiol* 80: 10F–19F, 1997.
10. **Persson PB.** Modulation of cardiovascular control mechanisms and their interaction. *Physiol Rev* 76: 193–244, 1996.
11. **Randall JE.** *Microcomputers and Physiological Simulation.* Reading, MA: Addison-Wesley, 1980.
12. **Rosenbaum DS, Albrecht P, and Cohen RJ.** Predicting sudden cardiac death from T wave alternans of the surface electrocardiogram: promise and pitfalls. *J Cardiovasc Electrophysiol* 7: 1095–1111, 1996.
13. **Ryan TJ, Antman EM, Brooks NH, Califf RM, Hillis LD, Hiratzka LF, Rapaport E, Riegel B, Russell RO, Smith EE, Weaver WD, Gibbons RJ, Alpert JS, Eagle KA, Gardner TJ, Garson A Jr, Gregoratos G, and Smith SC Jr.** 1999 Update: ACC/AHA guidelines for the management of patients with acute myocardial infarction: executive summary and recommendations: a Report of the American College of Cardiology/American Heart Association task force on practice guidelines (committee on management of acute myocardial infarction). *Circulation* 100: 1016–1030, 1999.
14. **Savard P, Rouleau JL, Ferguson J, Poitras N, Morel P, Davies RF, Stewart DJ, Talajic M, Gardner M, Dupuis R, Lauzon C, Sussex B, Potvin L, and Warnica W.** Risk stratification after myocardial infarction using signal-averaged elec-

- trocardiographic criteria adjusted for sex, age, and myocardial infarction location. *Circulation* 96: 202–213, 1997.
15. **Schmidt G, Malik M, Barthel P, Schneider R, Ulm K, Rolnitzky L, Camm AJ, Bigger JT Jr, and Schomig A.** Heart-rate turbulence after ventricular premature beats as a predictor of mortality after acute myocardial infarction. *Lancet* 353: 1390–1396, 1999.
  16. **Stein PK and Kleiger RE.** Insights from the study of heart rate variability. *Annu Rev Med* 50: 249–261, 1999.
  17. **Weber EH.** Über die Anwendung der Wellenlehre auf die Lehre vom Kreislaufe des Blutes und insbesondere auf die Pulslehre. In: *Berichte über die Verhandlungen der Königlich Sächsischen Gesellschaft der Wissenschaften zu Leipzig. Mathematisch-Physische Classe 1850* 3: 164–204, 1851.

